Final Report on Grant NAG1-946
Advanced Booster Guidance Studies

ICAM REPORT 93-03-01

Eugene M. Cliff

Aerospace and Ocean Engineering Department
and
Interdiscplinary Center for Applied Mathematics
Virginia Polytechnic Institute and State University
Blacksburg, VA 24061

March 1, 1993

Final Report on Grant NAG1-946

Advanced Booster Guidance Studies

Eugene M. Cliff

Aerospace and Ocean Engineering Department

and

Interdisciplinary Center for Applied Mathematics

Virginia Polytechnic Institute and State University

Blacksburg, VA 24061-0531

1 March 1993

This report is a summary of work done under **Grant NAG1-946** for the period 19 December 1988 through 15 August 1992. Most of the technical work is described in the papers produced, including the NASA Contractor Report 4393 - 'Optimal Control Problems with Switching Points'. In the following pages we present a list of the papers along with a brief abstract. The technical work during the last months of the grant has not yet been submitted for publication so we present a summary of that work in an Appendix.

Students Supported

In addition to the technical work a principal result of this work is the graduate study supported by it. The following students have been supported, in part, under this activity:

- Hans Seywald, Ph.D. student, Aerospace and Ocean Engineering Department.
- Pangiotas Tsiotras, Ph.D. student, Aerospace and Ocean Engineering Department.
- Diane DeWalt Smith, Ph.D. student, Aerospace and Ocean Engineering Department.
- Marwan Bikdash, Ph.D. student, Electrical Engineering Department.
- William Waldron, Ph.D. student, Aerospace and Ocean Engineering Department.

Papers Produced

H. Seywald and E.M. Cliff, 'Optimal Rocket-Powered Ascent Study', Proc. of the American Control Conference, Pittsburgh, PA, June 1989, pp. 2026-2031; also J. Guidance Control and Dynamics, to appear.

> The Goddard Problem is that of maximizing the final altitude for a vertically ascending, rocket-powered vehicle under the influence of an inverse square gravitational field and aerodynamic drag. The present paper is concerned with the effect of two additional constraints; a dynamic pressure limit (q_{max}) and a specified time of flight (t_f). Nine different switching structures involving zero-thrust (coasting) arcs, full-thrust arcs, singular-thrust (sustaining) arcs and state-constrained arcs are obtained for prescribed values of the parameters q_{max} and t_f. Finally, a comparison is given between the optimal thrust program and a simple intuitive feedback law.

E.M. Cliff, 'A Singular Perturbation Approach to Pitch-Loop Design', Proc. of the American Control Conference, San Diego, CA, May 1990, pp. 1819-1823

> Singular perturbation ideas are used to design a pitch-loop controller for a thrusting vehicle. The main feature of this approach is that the inner-loop design is based on a performance criterion that is consistent with the minimum-fuel index that was used in shaping the trajectory. The inner-loop design can be approximated by a linear-quadratic problem so that the resulting quadratic index is meaningful for fuel-efficient operation. The quadratic index that results is non-intuitive and features a control-state weighting term and zero-weight on the state itself. We define a coupling parameter that indicates when the state dynamics can be successfully separated into 'slow' and 'fast' categories.

H. Seywald, 'Optimal Control Problems with Switching Points', Ph.D. Dissertation, Virginia Polytechnic Institute and State University, Blacksburg, VA July 1990. (also NASA CR-4393)

H. Seywald, R.R. Kumar and E.M. Cliff, 'A New Proof of the Jacobi Necessary Condition', Proc. of the American Control Conference, Boston, MA, June 1991; also J. Guidance Control and Dynamics, to appear.

> Jacobi's necessary condition states that a minimizing extremal does not contain any conjugate points. This result has practical value because it enables one to discard any extremals that fail the conjugate point test. While the available proofs establish the theorem under the hypothesis that the test extremal is smooth, many applications give rise to non-smooth extremals. In this paper we present a proof that is valid for the case of extremals with corners.

H. Seywald and E.M. Cliff, 'A Feedback Control System for the Advanced Launch System', Proc. AIAA Guidance, Navigation and Control Conf., New Orleans, LA, August 1991, pp. 172-181.

A robust feedback algorithm is presented for near minimum-fuel ascent of a two stage vehicle operating in a vertical plane. The approach is based on neighboring optimal control ideas but employs feedback gains determined by finite differences applied to a family of extremals. Performance and robustness of the feedback law are found to be excellent.

H. Seywald, E.M. Cliff and K.-H. Well, 'Range Optimization for a Supersonic Aircraft', Proc. AIAA Guidance, Navigation and Control Conf., New Orleans, LA, August 1991, p 967-974.

Range-optimal trajectories for an aircraft flying in the vertical plane are determined form Pontryagin's Minimum Principle. Controls are the load factor, which appears nonlinearly in the model and the throttle, which appears only linearly. The controls are subject to fixed bounds and the state-inequality restricting the dynamic pressure is also imposed. The solutions contain state-constrained arcs and along these the controls are sometimes singular. A total of six different switching structures is found, depending on the value of the load-factor bound.

H. Seywald, 'Optimal Control Problems with Switching Points', NASA Contractor Report 4393, September 1991.

A brief discussion of existing optimality conditions is given and a numerical approach for solving the multipoint boundary value problems associated with the first-order optimality conditions is presented. Two realistic aerospace optimization problems are treated explicitly. these are altitude maximization for a sounding rocket (the Goddard Problem) in the presence of a dynamic pressure limit, and the range optimization for a supersonic aircraft in vertical plane flight, also in the presence of a dynamics pressure limit. An extension of the Generalized Legendre Clebsch condition to the case of singular control along a state/control constrained arc is presented and is applied to the aircraft range optimization problem.

Appendix
Optimal Ascent with Pitch Dynamics

by

William Waldron

Abstract

Optimal ascent paths for rocket-powered vehicles are commonly studied using point-mass models. In these formulations important gust-load constraints must be imposed in approximate form as q (dynamic-pressure) or q-α bounds. Thus, it is of interest to study these paths with more complete rigid-body models. In this section we begin with a review of the optimal ascent problem in point-mass approximation. The analysis is then extended to include pitch dynamics in boundary-layer approximation. The present effort includes the zeroth-order outer solution wherein the pitch dynamics are equilibrated and treated as algebraic equality constraints in the point-mass model. Future work will extend this to include the q-α dynamics in boundary-layer approximation and to compare these to numerical solutions with a full pitch-plane rigid body model.

Point Mass Model:

Mathematical Framework:

Equations of Motion

In order to analyze the trajectory of our launch vehicle we express our system by the mathematical model;

$$\dot{x} = f(x,u) \qquad x^T = (r,\phi,V,\gamma,m)$$

$$u^T = (\varepsilon)$$

where

- r = distance from center of earth to vehicle (radius)
- ϕ = downrange angle
- V = velocity of the vehicle
- γ = flight path angle of the vehicle
- m = vehicle mass

and

- ε = engine deflection with respect to body.

See Figure 1 for a depiction of these states variables.

The equations of motion are;

$$\dot{r} = V \cdot \sin\gamma$$

$$\dot{\phi} = \frac{V \cdot \cos\gamma}{r}$$

$$\dot{V} = \frac{T \cdot \cos\varepsilon - D}{m} - g \cdot \sin\gamma$$

$$\dot{\gamma} = \frac{T \cdot \sin\varepsilon + L}{m \cdot V} + \left(\frac{V}{r} - \frac{g}{V}\right) \cdot \cos\gamma$$

$$\dot{m} = -\frac{T_{vac}}{c}$$

where the gravitational acceleration is modeled as $g = g_0 \cdot \left(\frac{r_e}{r}\right)^2$.

These equations which are in dimensional form are often difficult to work with numerically. To alleviate some of the difficulties the equations are scaled and non-dimensionalized. This results in all the state variables having values near unity. The following scaling factors are used;

scale length:	$\bar{r} = r_e$	earth radius
scale mass:	$\bar{m} = m_0$	initial vehicle mass
scale acceleration:	$\bar{a} = g_0$	gravitational acceleration at surface

These scale factors lead to the following additional scale factors;

scale time: $\bar{t} = \sqrt{\frac{\bar{r}}{\bar{a}}}$

scale force: $\bar{f} = \frac{\bar{m} \cdot \bar{r}}{\bar{t}^2}$

scale velocity: $\bar{v} = \frac{\bar{r}}{\bar{t}}.$

If we now define our new non-dimensional variables as follows:

$$\hat{r} = \frac{r}{\bar{r}} \qquad \hat{T} = \frac{T}{\bar{f}}$$

$$\hat{\phi} = \phi \qquad \hat{D} = \frac{D}{\bar{f}}$$

$$\hat{V} = \frac{V}{\bar{v}} \qquad \hat{L} = \frac{L}{\bar{f}}$$

$$\hat{\gamma} = \gamma \qquad \hat{c} = \frac{c}{\bar{v}}$$

$$\hat{m} = \frac{m}{\bar{m}} \qquad \hat{\varepsilon} = \varepsilon.$$

Note that the variables that represent angular measurements are not modified.

The equations of motion can now be written in non-dimensional form. For reasons of visual clarity the "^" notation will be dropped from the non-dimensional variables. From this point on all variables will be non-dimensional unless otherwise noted. Our non-dimensional equations of motion are,

$$\dot{r} = V \cdot \sin\gamma$$

$$\dot{\phi} = \frac{V \cdot \cos\gamma}{r}$$

$$\dot{V} = \frac{T \cdot \cos\varepsilon - D}{m} - \frac{\sin\gamma}{r^2}$$

$$C_L(M,\alpha) = C_{L_\alpha}(M)\cdot(\alpha\cdot\tfrac{180}{\pi})$$

$$C_{L_\alpha}(M) = C_1(M) + C_2(M) + C_3(M)$$

$$C_1(M) = C_{10} + C_{11}\cdot\tan^{-1}(C_{12}\cdot M - C_{13})$$

$$C_2(M) = C_{21}\cdot e^{(C_{22}\cdot(M-C_{23})^2)}$$

$$C_3(M) = C_{30} + C_{31}\cdot\tan^{-1}(C_{32}\cdot M - C_{33})$$

with function coefficients given in Tables 1 and 2.

In order to simplify the point mass model, the angle of attack dependence has been removed by holding α=0 throughout the trajectory. It has been shown for this vehicle that if the angle of attack is varied between plus and minus ten degrees the variation in all aerodynamic forces constitutes less than 1% of the total force acting on the vehicle.[2] A plot of the drag coefficient, C_D, vs. Mach number at α=0 is shown in Figure 2.

Atmospheric Model

The atmospheric model us such that the speed of sound, a[m/s], and density, ρ[kg/m^3], are given by the following relations;

$$a[\tfrac{m}{s}] = a_0\cdot\left[c_o + h\cdot c_1 + h^2\cdot c_2 + h\cdot c^3 + h\cdot c^4 + h\cdot c^5 + h\cdot c^6\right]$$

$$\rho[\tfrac{kg}{m^3}] = b_3\cdot e^{\left[-b_1 - h\cdot b_2 + b_1\cdot e^{\left[-(h\cdot a_1 + h^2\cdot a_2 + h^3\cdot a_3 + h^4\cdot a_4)\right]}\right]}$$

where h is the altitude in kilometers and the function coefficients are given in Tables 4 and 5.

Optimization Approach:

Problem Statement

The task at hand is to launch the vehicle into an orbit with a specified semi-major axis and orbit eccentricity using the least amount of fuel. These terminal conditions can be defined by the following constraints.

$$\psi_1 = \frac{2}{r(t_f)} - V(t_f)^2 - \frac{1}{a} = 0$$

$$\psi_2 = \cos^2\gamma(t_f)\cdot\left[V(t_f)^4\cdot r(t_f)^2 - 2\cdot V(t_f)^2\cdot r(t_f)\right] + 1 - e^2 = 0$$

where a is the desired semi-mafor axis and e is the desired orbit eccentricity.

In addition to these constraints on the state variables at final time, there are also constraints on the mass at staging;

$$\psi_3 = m(t_s^-) - m_s^- = 0$$

$$\psi_4 = (m_s^- - \Delta m_s) - m(t_s^+) = 0$$

where m_s^- is the desired vehicle mass before staging, Δm_s is the desired change in vehicle mass at staging, $m(t_s^-)$ is the vehicle mass before staging, and $m(t_s^+)$ is the vehicle mass after staging. At staging the aerodynamics of the vehicle change, but the dynamic pressure has dropped off significantly resulting in this change having negligible effect on the trajectory. For this reason the aerodynamic model does not change at staging which results in a simplification of the simulation.

We can now define our cost or performance index, J, as;

$$J = -m(t_f).$$

Hamiltonian

To solve the optimal control problem we shall employ the Minimum Principle. Accordingly we define the usual variational Hamiltonian.

$$H = \lambda^T \cdot f(x,u) = \lambda_r \cdot [V \cdot \sin\gamma] + \lambda_\phi \cdot \left[\frac{V \cdot \cos\gamma}{r}\right] + \lambda_V \cdot \left[\frac{T \cdot \cos\varepsilon - D}{m} - \frac{\sin\gamma}{r^2}\right]$$

$$+\lambda_\gamma \cdot \left[\frac{T \cdot \sin\varepsilon + L}{m \cdot V} + \left(\frac{V}{r} - \frac{1}{V \cdot r^2}\right) \cdot \cos\gamma\right] + \lambda_m \cdot \left[-\frac{T_{vac}}{c}\right]$$

Costate Differential Equations

The differential equations for the costates are given by the relation,

$$\dot{\lambda}_i = -\frac{\partial H}{\partial x_i}.$$

For our problem this results in the following differential equations for the costates:

$$\dot{\lambda}_r = \lambda_\phi \cdot \left[\frac{V \cdot \cos\gamma}{r^2}\right] - \lambda_V \cdot \left[\frac{T_r \cdot \cos\varepsilon - D_r}{m} + \frac{2\sin\gamma}{r^3}\right]$$

$$-\lambda_\gamma \cdot \left[\frac{T_r \cdot \sin\varepsilon + L_r}{m \cdot V} - \left(\frac{V}{r^2} - \frac{2}{V \cdot r^3}\right) \cdot \cos\gamma\right]$$

$$\dot{\lambda}_\phi = 0$$

$$\dot{\lambda}_V = -\lambda_r \cdot [\sin\gamma] - \lambda_\phi \cdot \left[\frac{\cos\gamma}{r}\right] + \lambda_V \cdot \left[\frac{D_V}{m}\right]$$

$$-\lambda_\gamma \cdot \left[\frac{L_V}{m \cdot V} - \frac{T \cdot \sin\varepsilon + L}{m \cdot V^2} + \left(\frac{1}{r} + \frac{1}{V^2 \cdot r^2}\right) \cdot \cos\gamma\right]$$

$$\dot{\lambda}_\gamma = -\lambda_r \cdot [V \cdot \cos\gamma] + \lambda_\phi \cdot \left[\frac{V \cdot \sin\gamma}{r}\right] + \lambda_V \cdot \left[\frac{\cos\gamma}{r^2}\right]$$

$$+\lambda_\gamma \cdot \left[\left(\frac{V}{r} - \frac{1}{V \cdot r^2}\right) \cdot \sin\gamma\right]$$

$$\dot{\lambda}_m = \lambda_V \cdot \left[\frac{T \cdot \cos\varepsilon - D}{m^2}\right] + \lambda_\gamma \cdot \left[\frac{T \cdot \sin\varepsilon + L}{m^2 \cdot V}\right]$$

Control Calculation

Our control, u(t), can be determined by looking for a u(t) that minimizes the Hamiltonian. We can find such a control by setting $\frac{\partial H}{\partial u} = 0$ and solving for u(t).

$$\frac{\partial H}{\partial u} = \frac{\partial H}{\partial \varepsilon} = -\lambda_V \cdot \frac{T \cdot \sin\varepsilon}{m} + \lambda_\gamma \cdot \frac{T \cdot \cos\varepsilon}{m \cdot V} = 0$$

$$\lambda_V \cdot \sin\varepsilon = \lambda_\gamma \cdot \frac{\cos\varepsilon}{V}$$

$$\tan\varepsilon = \frac{\lambda_\gamma / V}{\lambda_V}$$

This gives our control, u(t)=ε(t), as a function of the costates λ_γ and λ_V as well as the state variable V. There is still a quadrant resolution problem to be solved. In order to resolve the ambiguity we require that $\frac{\partial^2 H}{\partial \varepsilon^2} \geq 0$. This leads to the expression:

$$-\lambda_V \cos\varepsilon - \lambda_\gamma \frac{\sin\varepsilon}{V} \geq 0.$$

Using this expression the correct quadrant for our control, ε, is specified.

Terminal Conditions

We now need to determine the terminal conditions on our costates. To do so we define a function, Φ, made up of our cost function and the dot product of constant multipliers, υ_i, and our terminal and staging conditions ψ_i.

$$\Phi = J + \upsilon^T \cdot \psi = -m(t_f) + \upsilon_1 \cdot \left[\frac{2}{r(t_f)} - V(t_f)^2 - \frac{1}{a}\right]$$

$$+\upsilon_2 \cdot \left[\cos^2\gamma(t_f) \cdot \left[V(t_f)^4 \cdot r(t_f)^2 - 2 \cdot V(t_f)^2 \cdot r(t_f)\right] + 1 - e^2\right]$$

$$+\upsilon_3 \cdot \left[m(t_s^-) - m_s^-\right] + \upsilon_4 \cdot \left[(m_s^- - \Delta m_s) - m(t_s^+)\right]$$

The boundary conditions on our costates at final time are determined by the relation; $\lambda_i(t_f) = \frac{\partial \Phi}{\partial x_i(t_f)}$. Our terminal conditions on the costates become

$$\lambda_r(t_f) = -\upsilon_1 \cdot \left[\frac{2}{r(t_f)^2}\right] + \upsilon_2 \cdot \left[\cos^2\gamma(t_f) \cdot \left[2 \cdot V(t_f)^4 \cdot r(t_f) - 2 \cdot V(t_f)^2\right]\right]$$

$$\lambda_\phi(t_f) = 0$$

$$\lambda_V(t_f) = \upsilon_1 \cdot \left[-2 \cdot V(t_f)\right] + \upsilon_2 \cdot \left[\cos^2\gamma(t_f) \cdot \left[4 \cdot V(t_f)^3 \cdot r(t_f)^2 - 4 \cdot V(t_f) \cdot r(t_f)\right]\right]$$

$$\lambda_\gamma(t_f) = \upsilon_2 \cdot \left[-2 \cdot \cos\gamma(t_f) \cdot \sin\gamma(t_f) \cdot \left[V(t_f)^4 \cdot r(t_f)^2 - 2 \cdot V(t_f)^2 \cdot r(t_f)\right]\right]$$

$$\lambda_m(t_f) = -1$$

In addition, since our final time is unspecified: $H(t_f) = 0$.

Staging Conditions

When the launch vehicle reaches a specified value of mass, m_s^-, staging occurs. During staging, which is assumed to occur instantaneously in our model, the vehicle mass is reduced by a specified value of Δm_s. In addition to the change in the state variable, m, the corresponding costate also is discontinuous. The values of our costate both before and after staging are given by the following relations [3];

$$\lambda_m(t_s^-) = \frac{\partial \Phi}{\partial m(t_s^-)}$$

$$\lambda_m(t_s^+) = -\frac{\partial \Phi}{\partial m(t_s^+)}$$

which leads to the conditions;

$$\lambda_m(t_s^-) = \upsilon_3$$

$$\lambda_m(t_s^+) = \upsilon_4.$$

Since both υ_3 and υ_4 are arbitrary, these two relations can be reduced to

$$\lambda_m(t_s^+) - \lambda_m(t_s^-) = \Delta\lambda_m(t_s)$$

where $\Delta\lambda_m(t_s)$ is an unknown to be determined. We also know that the value of the Hamiltonian, H, does not change during staging.

$$H(t_s^+) - H(t_s^-) = 0$$

Multi-Point Boundary Value Problem

Our problem is now a multi-point boundary value problem. Our known values at initial time, t_0=0, are

$$r(0) = r_0$$

$$\phi(0) = \phi_0$$

$$V(0) = V_0$$

$$\gamma(0) = \gamma_0$$

$$m(0) = m_0$$

with $m(t_s^+) = m(t_s^-) + \Delta m_s$ at staging.

The above problem needs to be solved using the state and costate differential equations for the following nine unknowns,

$\lambda_r(0)$, $\lambda_\phi(0)$, $\lambda_V(0)$, $\lambda_\gamma(0)$, $\lambda_m(0)$, t_f, $\Delta\lambda_m(t_s)$, υ_1, υ_2, to meet the following nine conditions.

(1) $$\lambda_r(t_f) = -\upsilon_1 \cdot \left[\frac{2}{r(t_f)^2}\right] + \upsilon_2 \cdot \left[\cos^2\gamma(t_f) \cdot \left[2 \cdot V(t_f)^4 \cdot r(t_f) - 2 \cdot V(t_f)^2\right]\right]$$

(2) $$\lambda_\phi(t_f) = 0$$

(3) $$\lambda_V(t_f) = \upsilon_1 \cdot \left[-2 \cdot V(t_f)\right] + \upsilon_2 \cdot \left[\cos^2\gamma(t_f) \cdot \left[4 \cdot V(t_f)^3 \cdot r(t_f)^2 - 4 \cdot V(t_f) \cdot r(t_f)\right]\right]$$

(4) $$\lambda_\gamma(t_f) = \upsilon_2 \cdot \left[-2 \cdot \cos\gamma(t_f) \cdot \sin\gamma(t_f) \cdot \left[V(t_f)^4 \cdot r(t_f)^2 - 2 \cdot V(t_f)^2 \cdot r(t_f)\right]\right]$$

(5) $\lambda_m(t_f) = -1$

(6) $H(t_s^+) - H(t_s^-) = 0$

(7) $$\frac{2}{r(t_f)} - V(t_f)^2 - \frac{1}{a} = 0$$

(8) $$\cos^2\gamma(t_f)\cdot\left[V(t_f)^4\cdot r(t_f)^2 - 2\cdot V(t_f)^2\cdot r(t_f)\right] + 1 - e^2 = 0$$

(9) $H(t_f) = 0.$

Point Mass Solution

The above problem was solved using Newton's method to find the nine unknowns. The solution converges rapidly once the initial guess for the unknowns are sufficiently close to the solution. The resulting control history, $\varepsilon(t)$ vs. time, can be seen in Figure 3. Time histories of the state and costate variables can be found in Figures 4 - 10.

Pitch Plane Model:

Mathematical Framework:

Equations of Motion

As before, in order to analyze the trajectory of our launch vehicle we express our system by a mathematical model;

$$\dot{x} = f(x, y, u) \qquad x^T = (r, \phi, V, \gamma, m)$$

$$\delta\dot{y} = g(x, y, u) \qquad y^T = (\theta, q)$$

$$u^T = (\varepsilon)$$

Our first set of state variables, x, are the same as in the point mass model and our new state variables, y, are the variables necessary to model the pitch plane.

θ = angular position of vehicle w.r.t local horizontal

q = angular rate of vehicle in pitch plane

The equations of motion for the pitch plane model are;

$$\dot{r} = V\cdot\sin\gamma$$

$$\dot{\phi} = \frac{V\cdot\cos\gamma}{r}$$

$$\dot{V} = \frac{T\cdot\cos(\theta - \gamma + \varepsilon) - D}{m} - \frac{\sin\gamma}{r^2}$$

$$\dot{\gamma} = \frac{T \cdot \sin(\theta - \gamma + \varepsilon) + L}{m \cdot V} + \left(\frac{V}{r} - \frac{1}{V \cdot r^2}\right) \cdot \cos\gamma$$

$$\dot{m} = -\frac{T_{vac}}{c}$$

$$\delta\dot{\theta} = q$$

$$\delta\dot{q} = \frac{M - T \cdot \ell \cdot \sin\varepsilon}{I_{yy}}$$

Aerodynamic Model

The pitch plane model necessitates the addition of pitching moment data into our model. The pitching moment about the center of mass is given as

$$M = \bar{q} \cdot S \cdot c \cdot C_M.$$

The moment coefficient is a function of Mach number and angle of attack and is surface fit by the relation;

$$C_M(M,\alpha) = L(M,\alpha) + E(M,\alpha)$$

$$L(M,\alpha) = L_1 \cdot M \cdot \left(\alpha \cdot \tfrac{180}{\pi}\right) + L_2 \cdot \left(\alpha \cdot \tfrac{180}{\pi}\right) + L_3 \cdot M + L_4$$

$$E(M,\alpha) = \left(E_1 \cdot \left(\alpha \cdot \tfrac{180}{\pi}\right) + E_2\right) \cdot e^{(\arg(M))}$$

$$\arg(M) = -\left(\frac{(M - M_0) \cdot \left(M_1 - \tan^{-1}\left(M_2 \cdot (M - M_0)\right)/\pi\right)}{\omega}\right)^2$$

Plots of the surface fitted aerodynamic coefficients C_D, C_L, and C_M can be seen in Figures 11, 12, and 13.

Pitch Moment of Inertia

The pitch moment of inertia for the launch vehicle is varied linearly as a function of vehicle mass.

Reduced Order Model:

Equilibrium Constraints

In order to ease the transition from the point mass model to a pitch plane model we will first look at a reduced order pitch plane model. This is implimented by letting our time scale variable, δ, go to zero in the above model. This implies that g(x,y,u) = 0 and our pitch plane variables θ and q become "control like". The resulting pitch plane constraints are;

$$q = 0$$

$$\frac{M - T \cdot \ell \cdot \sin\varepsilon}{I_{yy}} = 0.$$

Hamiltonian

We again employ the Minimum Principle and define our variational Hamiltonian.

$$H = \lambda_r \cdot [V \cdot \sin\gamma] + \lambda_\phi \cdot \left[\frac{V \cdot \cos\gamma}{r}\right] + \lambda_V \cdot \left[\frac{T \cdot \cos(\theta - \gamma + \varepsilon) - D}{m} - \frac{\sin\gamma}{r^2}\right]$$

$$+\lambda_\gamma \cdot \left[\frac{T \cdot \sin(\theta - \gamma + \varepsilon) + L}{m \cdot V} + \left(\frac{V}{r} - \frac{1}{V \cdot r^2}\right) \cdot \cos\gamma\right] + \lambda_m \cdot \left[-\frac{T_{vac}}{c}\right]$$

$$+\upsilon_\theta \cdot [q] + \upsilon_q \cdot \left[\frac{M - T \cdot \ell \cdot \sin\varepsilon}{I_{yy}}\right]$$

Costate Differential Equations

The costate differential equations are;

$$\dot{\lambda}_r = \lambda_\phi \cdot \left[\frac{V \cdot \cos\gamma}{r^2}\right] - \lambda_V \cdot \left[\frac{T_r \cdot \cos(\theta - \gamma + \varepsilon) - D_r}{m} + \frac{2\sin\gamma}{r^3}\right]$$

$$-\lambda_\gamma \cdot \left[\frac{T_r \cdot \sin(\theta - \gamma + \varepsilon) + L_r}{m \cdot V} - \left(\frac{V}{r^2} - \frac{2}{V \cdot r^3}\right) \cdot \cos\gamma\right]$$

$$-\upsilon_q \cdot \left[\frac{M_r - T_r \cdot \ell \cdot \sin\varepsilon}{I_{yy}}\right]$$

$$\dot{\lambda}_\phi = 0$$

$$\dot{\lambda}_V = -\lambda_r \cdot [\sin\gamma] - \lambda_\phi \cdot \left[\frac{\cos\gamma}{r}\right] + \lambda_V \cdot \left[\frac{D_V}{m}\right]$$

$$-\lambda_\gamma \cdot \left[\frac{L_V}{m \cdot V} - \frac{T \cdot \sin(\theta - \gamma + \varepsilon) + L}{m \cdot V^2} + \left(\frac{1}{r} + \frac{1}{V^2 \cdot r^2}\right) \cdot \cos\gamma\right]$$

$$-\upsilon_q \cdot \left[\frac{M_V}{I_{yy}}\right]$$

$$\dot{\lambda}_\gamma = -\lambda_r \cdot [V \cdot \cos\gamma] + \lambda_\phi \cdot \left[\frac{V \cdot \sin\gamma}{r}\right] - \lambda_V \cdot \left[\frac{T \cdot \sin(\theta - \gamma + \varepsilon) - D_\gamma}{m} - \frac{\cos\gamma}{r^2}\right]$$

$$+\lambda_\gamma \cdot \left[\frac{T \cdot \cos(\theta - \gamma + \varepsilon) - L_\gamma}{m \cdot V} + \left(\frac{V}{r} - \frac{1}{V \cdot r^2}\right) \cdot \sin\gamma\right] - \upsilon_q \cdot \left[\frac{M_\gamma}{I_{yy}}\right]$$

$$\dot{\lambda}_m = \lambda_V \cdot \left[\frac{T \cdot \cos(\theta - \gamma + \varepsilon) - D}{m^2}\right] + \lambda_\gamma \cdot \left[\frac{T \cdot \sin(\theta - \gamma + \varepsilon) + L}{m^2 \cdot V}\right]$$

$$+\upsilon_q \cdot \left[I_{yy_m} \cdot \frac{M - T \cdot \ell \cdot \sin\varepsilon}{I_{yy}^{\,2}}\right]$$

Control Calculation

We again set the derivative of the Hamiltonian with respect to each control to zero.

$$H_\theta = \lambda_V \cdot \frac{-T \cdot \sin(\theta - \gamma + \varepsilon) - D_\theta}{m} + \lambda_\gamma \cdot \frac{T \cdot \cos(\theta - \gamma + \varepsilon) + L_\theta}{m \cdot V} + \upsilon_q \cdot \frac{M_\theta}{I_{yy}} = 0$$

$$H_q = \upsilon_\theta = 0$$

$$H_\varepsilon = \lambda_V \cdot \frac{-T \cdot \sin(\theta - \gamma + \varepsilon)}{m} + \lambda_\gamma \cdot \frac{T \cdot \cos(\theta - \gamma + \varepsilon)}{m \cdot V} - \upsilon_q \cdot \frac{T \cdot \ell \cdot \cos\varepsilon}{I_{yy}} = 0$$

The above three equations along with the two pitch equilibrium equations need to be solved for the five unknowns; q, θ, ε, υ_q, and υ_θ. It can easily be seen that the variables q and υ_θ are equal to zero and decouple from the rest of the system. Therefore the problem of solving for our control reduces to a system of three equations and three unknowns.

$$\frac{M - T \cdot \ell \cdot \sin\varepsilon}{I_{yy}} = 0.$$

$$H_\theta = \lambda_V \cdot \frac{-T \cdot \sin(\theta - \gamma + \varepsilon) - D_\theta}{m} + \lambda_\gamma \cdot \frac{T \cdot \cos(\theta - \gamma + \varepsilon) + L_\theta}{m \cdot V} + \upsilon_q \cdot \frac{M_\theta}{I_{yy}} = 0$$

$$H_\varepsilon = \lambda_V \cdot \frac{-T \cdot \sin(\theta - \gamma + \varepsilon)}{m} + \lambda_\gamma \cdot \frac{T \cdot \cos(\theta - \gamma + \varepsilon)}{m \cdot V} - \upsilon_q \cdot \frac{T \cdot \ell \cdot \cos\varepsilon}{I_{yy}} = 0$$

The above equations are nonlinear and must be solved iteratively for the unknowns throughout the trajectory.

Multi-Point Boundary Value Problem

Since the reduced order model does not introduce any new state variables, θ and q are treated as controls, the initial, staging, and terminal conditions are the same as in the point mass boundary value problem.

Shooting Point Technique

With added complexity of the pitch plane model numerical difficulties start to arise. These difficulties are a result of integrating the costate differential equations which are unstable. To work around the instabilities the intervals both before and after staging are broken down into several smaller intervals. The idea is to have the intervals small enough so that the unstable costates do not "blow up" before the end of the interval is reached.

At the beginning of the next the costates are reset to new initial values and the integration is continued. After the integration is complete for the entire trajectory the initial values for each interval are adjusted in an attempt to match end conditions on each interval as well as the boundary conditions for the entire problem. This technique is useful in alleviating some of the numerical instabilities but results in a larger Newton problem with more unknowns.

Reduced Order Pitch Plane Solution

The control history, $\varepsilon(t)$ vs. time, and angle of attack history, $\alpha(t)$ vs. time, for the optimal trajectory can be found in Figures 14 and 15 respectively. Time histories of the state and costate variables can be found in Figures 16 - 22.

Tables:

c_0	0.187	k_0	0.001075
c_{10}	0.5	k_{10}	0.5
c_{11}	0.3410828	k_{11}	0.508753
c_{12}	10.0	k_{12}	-0.5
c_{13}	8.5	k_{13}	-1.5
c_{20}	0.43	k_{20}	0.00015
c_{21}	0.28	k_{21}	0.00055
c_{22}	-1.15	k_{22}	-1.5
c_{23}	0.75	k_{23}	2.5

Table 1: Coefficients for C_D functionalization

c_{10}	0.05119
c_{11}	0.0050695
c_{12}	1.2
c_{13}	4.32
c_{21}	-0.002
c_{22}	-1.7
c_{23}	1.75
c_{30}	-0.005
c_{31}	0.0040915
c_{32}	-0.25
c_{33}	-2.75

Table 2: Coefficients for C_L functionalization

L_1	$-0.27101094838599 \times 10^{-3}$
L_2	$+0.11682570862606 \times 10^{-1}$
L_3	$+0.16851032948609 \times 10^{-2}$
L_4	$+0.35751730216124 \times 10^{-2}$
E_1	$+0.31816920579938 \times 10^{-2}$
E_2	$+0.35019268019610 \times 10^{-1}$
M_0	$+0.13713067220255 \times 10^{+1}$
M_1	1.5
M_2	$1.0 \times 10^{+6}$
ω	+0.84593773937827

Table 3: Coefficients for C_M functionalization

a_0	+332.9494352
c_0	+1.02207711387
c_1	$-0.262500934305 \times 10^{-1}$
c_2	$+0.142474099963 \times 10^{-2}$
c_3	$-0.29840490767 9 \times 10^{-4}$
c_4	$+0.274897035390 \times 10^{-6}$
c_5	$-0.109152741878 \times 10^{-8}$
c_6	$+0.147617851753 \times 10^{-11}$

Table 4: Coefficients for speed of sound model

b_1	+1.0228055
b_2	+0.12122693
b_3	+1.225
a_1	$-3.48643241 \times 10^{-2}$
a_2	$+3.50991865 \times 10^{-3}$
a_3	$-8.33000535 \times 10^{-5}$
a_4	$+1.15219733 \times 10^{-6}$

Table 5: Coefficients for density model

References

1. Pamadi, B., Spacecraft Control Branch, NASA Langley Research Center, Hampton, VA., private communication.

2. Seywald, H. and Cliff, E.M., "A Feedback Control for the Advanced Launch System".

3. Bryson, A.E. and Ho, Y., Applied Optimal Control, Hemisphere Publishing Corporation, 1975.

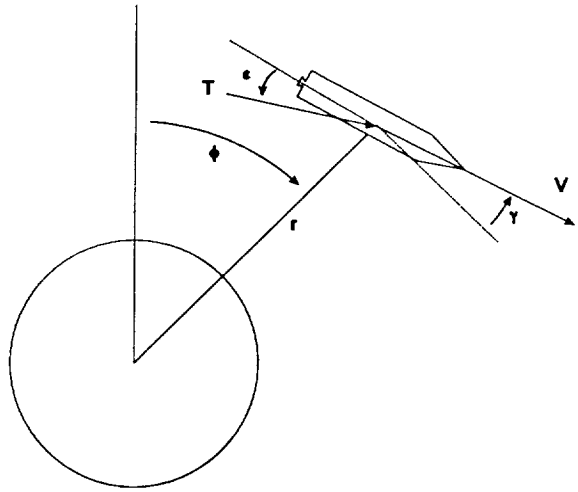

Figure 1: State Variable Depiction

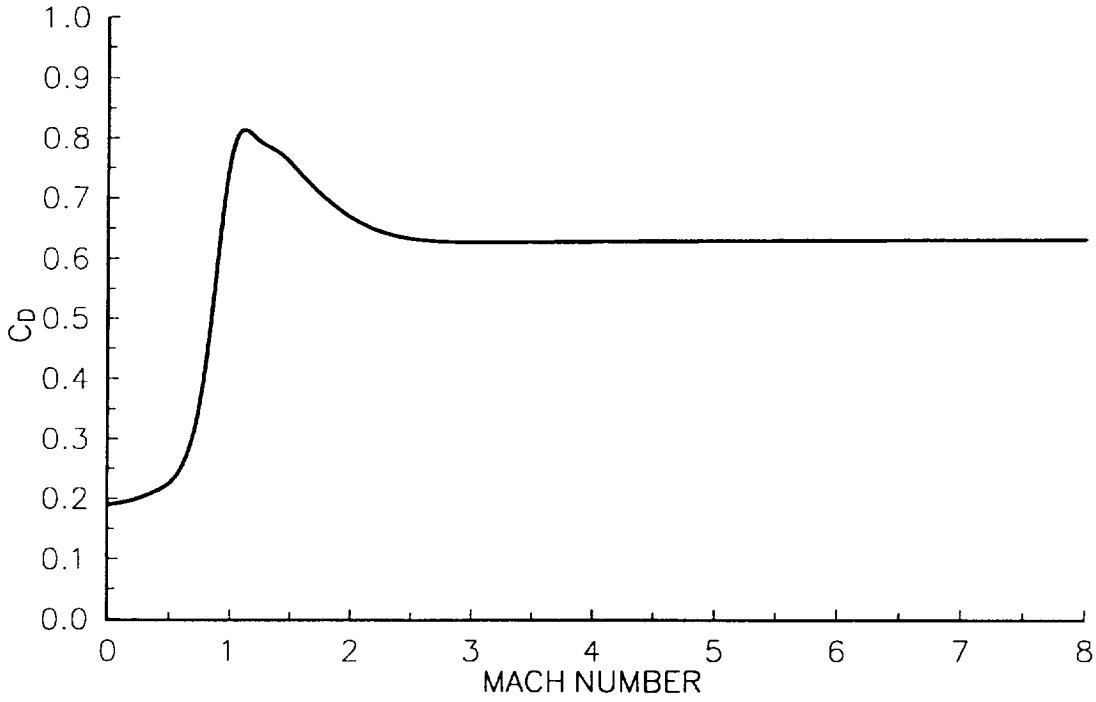

Figure 2: Drag Coefficient vs. Mach Number at α=0.0

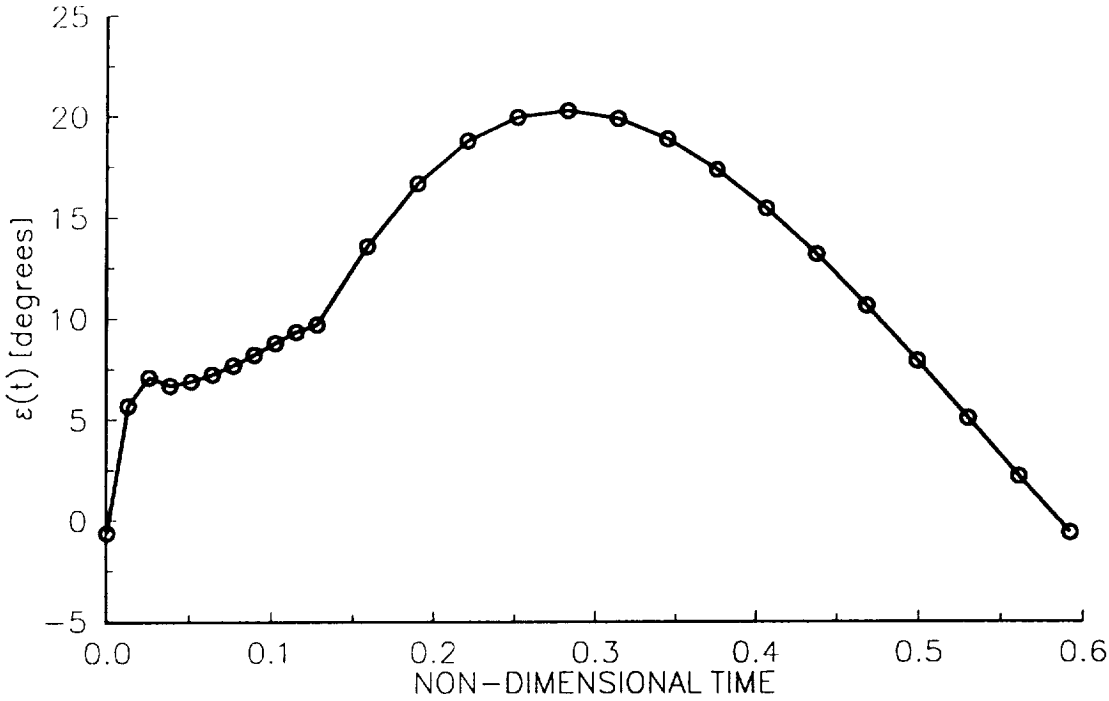

Figure 3: Control History, $\varepsilon(t)$, for Point Mass Solution

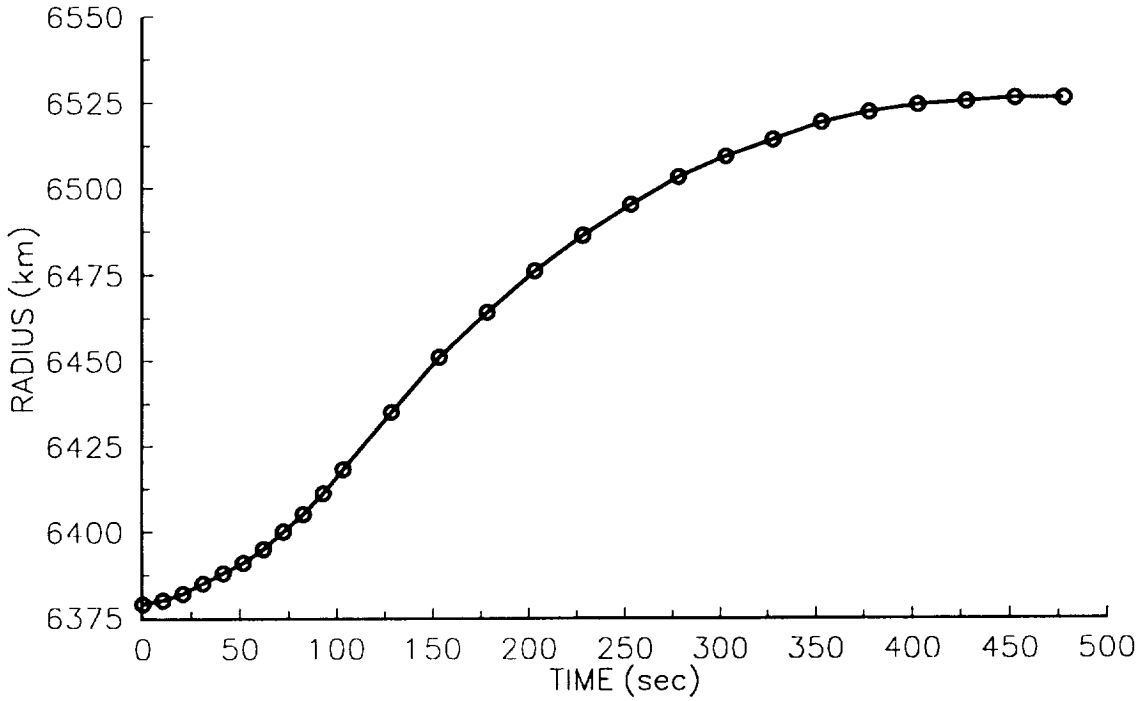

Figure 4: Radius History for Point Mass Solution

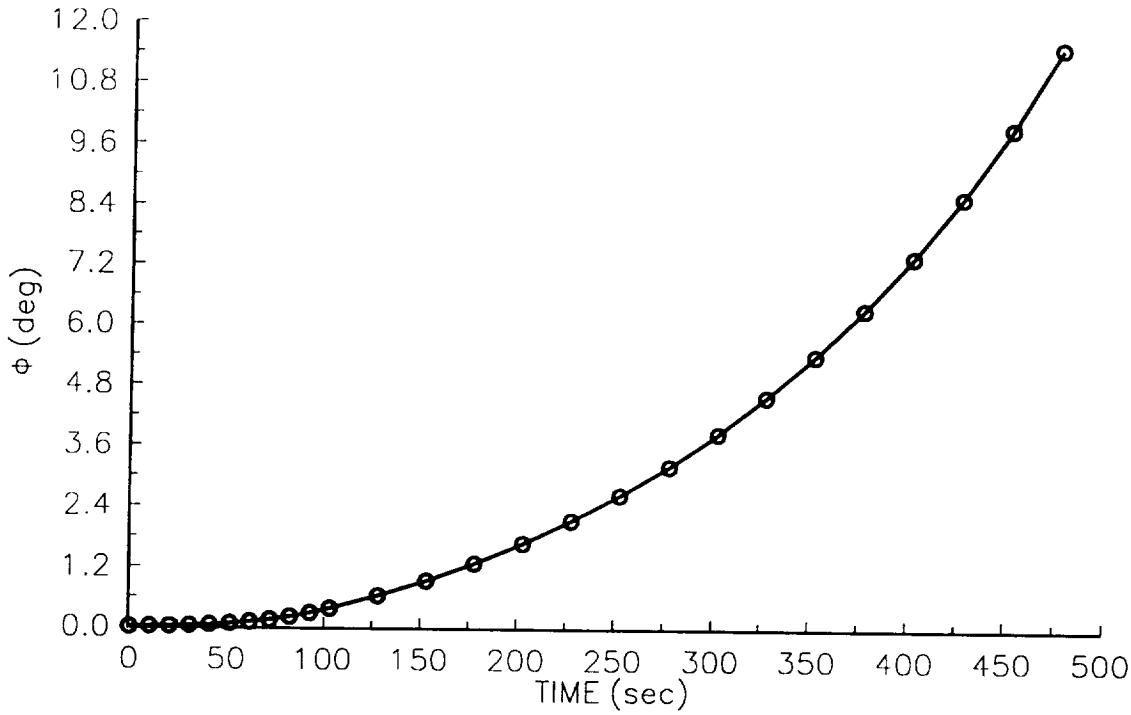

Figure 5: Downrange Angle for Point Mass Solution

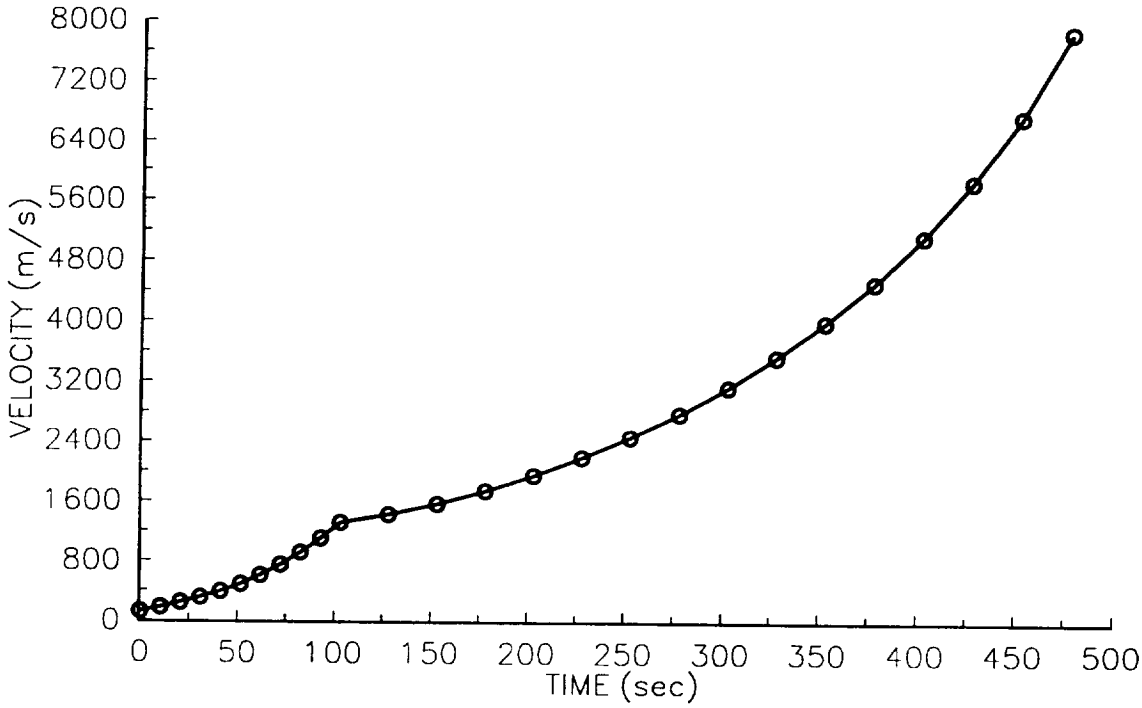

Figure 6: Velocity History for Point Mass Solution

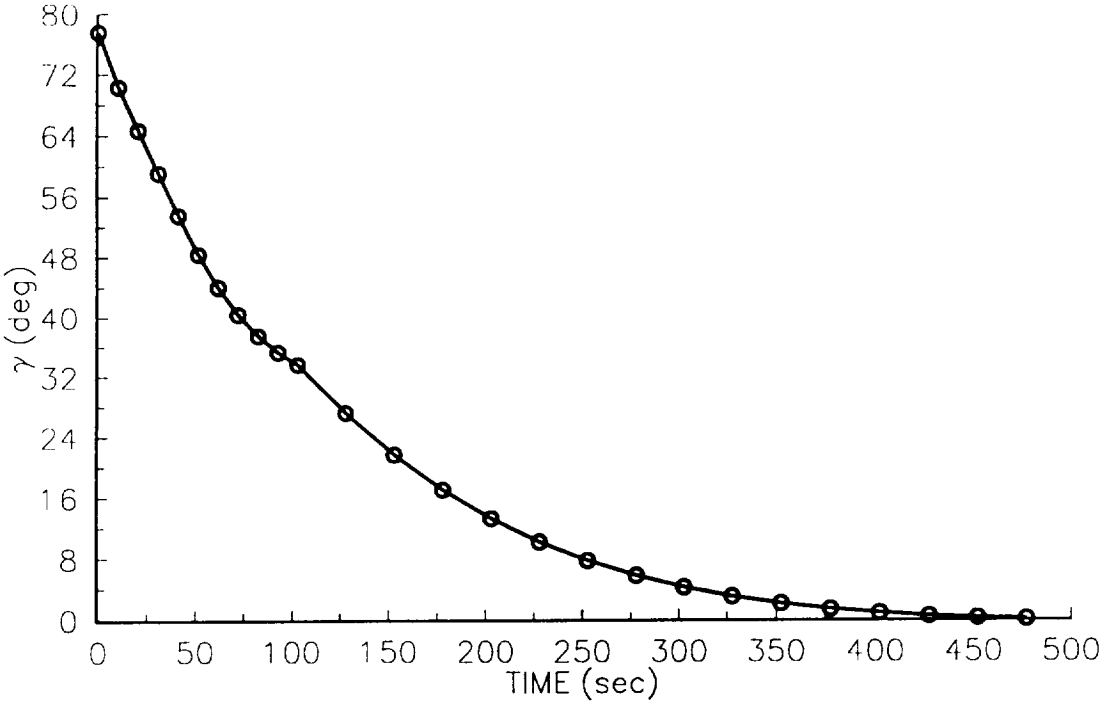

Figure 7: Flight Path Angle for Point Mass Solution

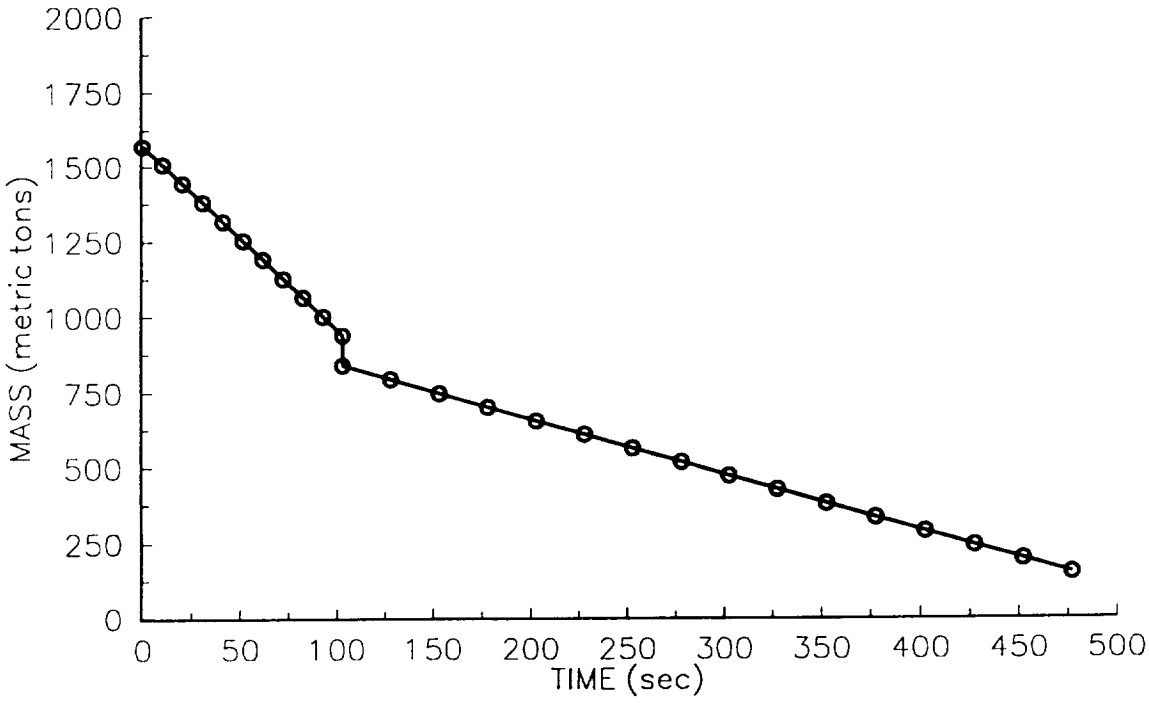

Figure 8: Vehicle Mass History for Point Mass Solution

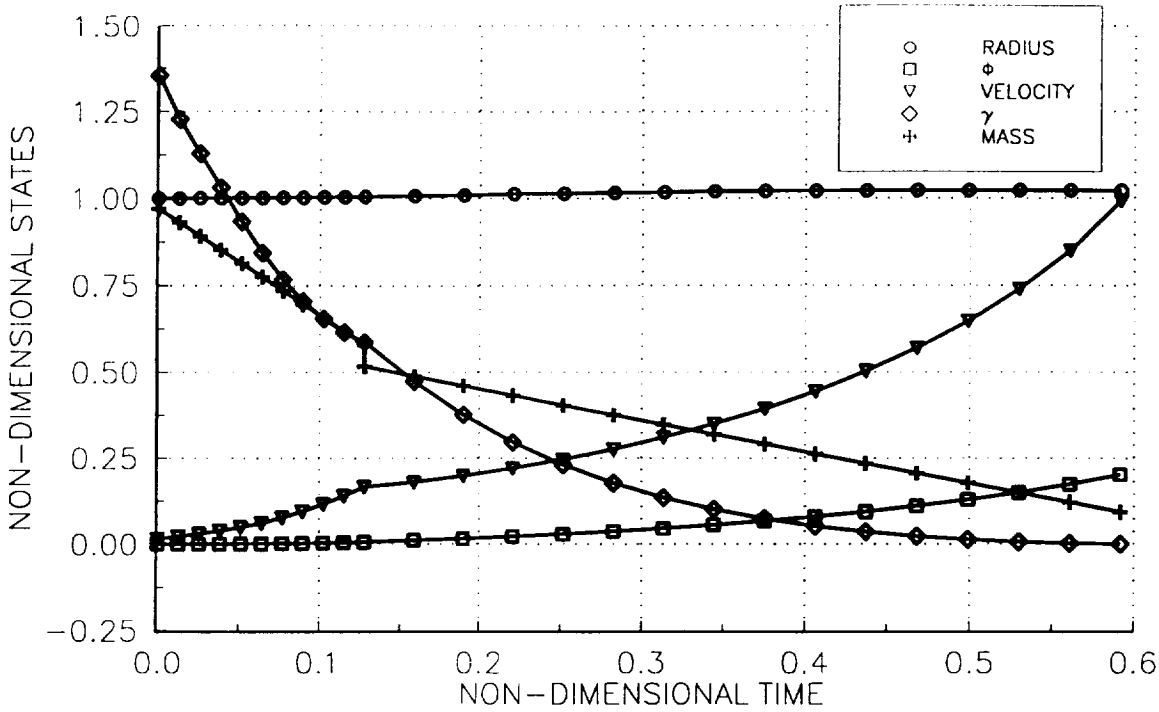

Figure 9: State Variables for Point Mass Model

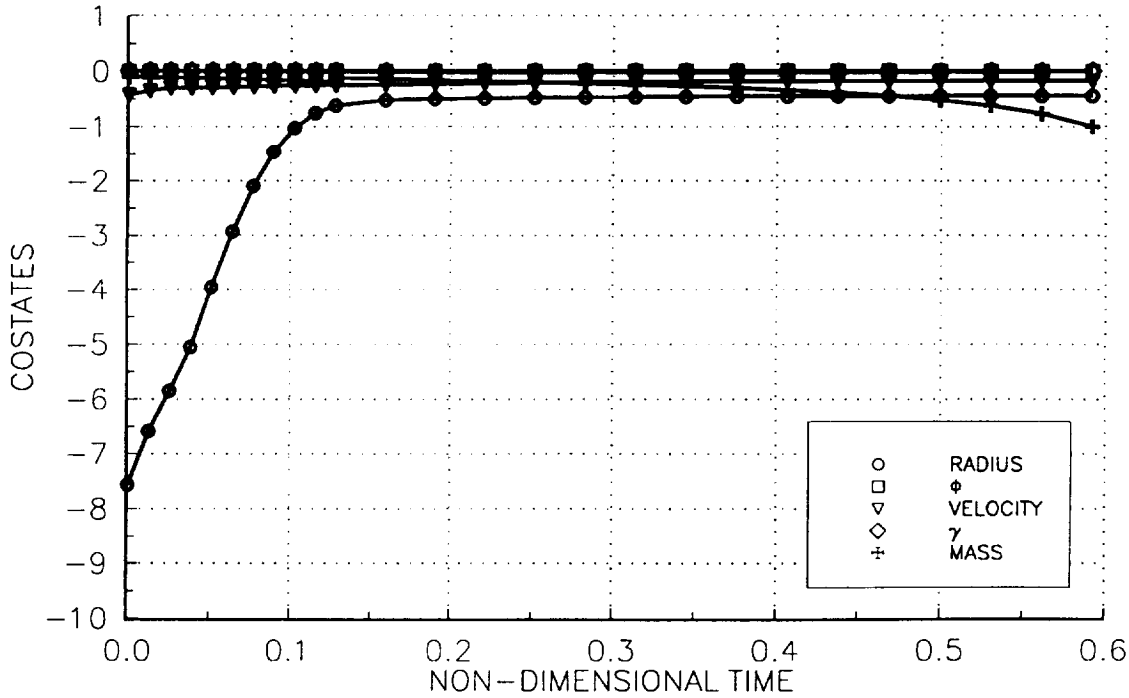

Figure 10: Costate Variables for Point Mass Solution

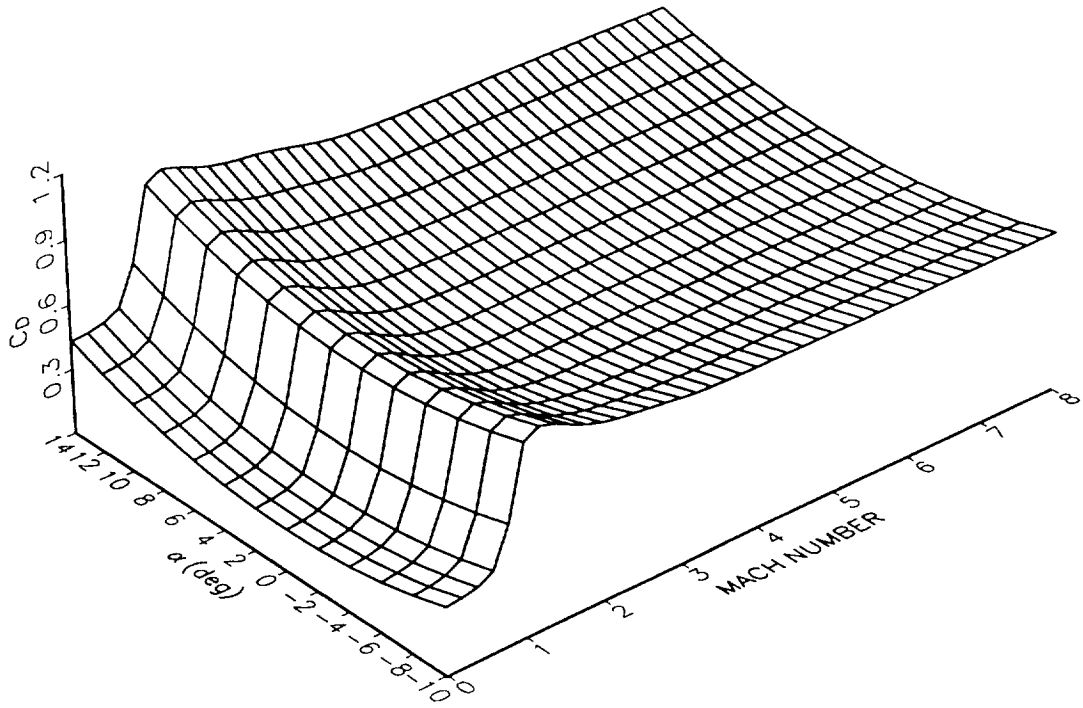

Figure 11: Drag Coefficient Surface Plot

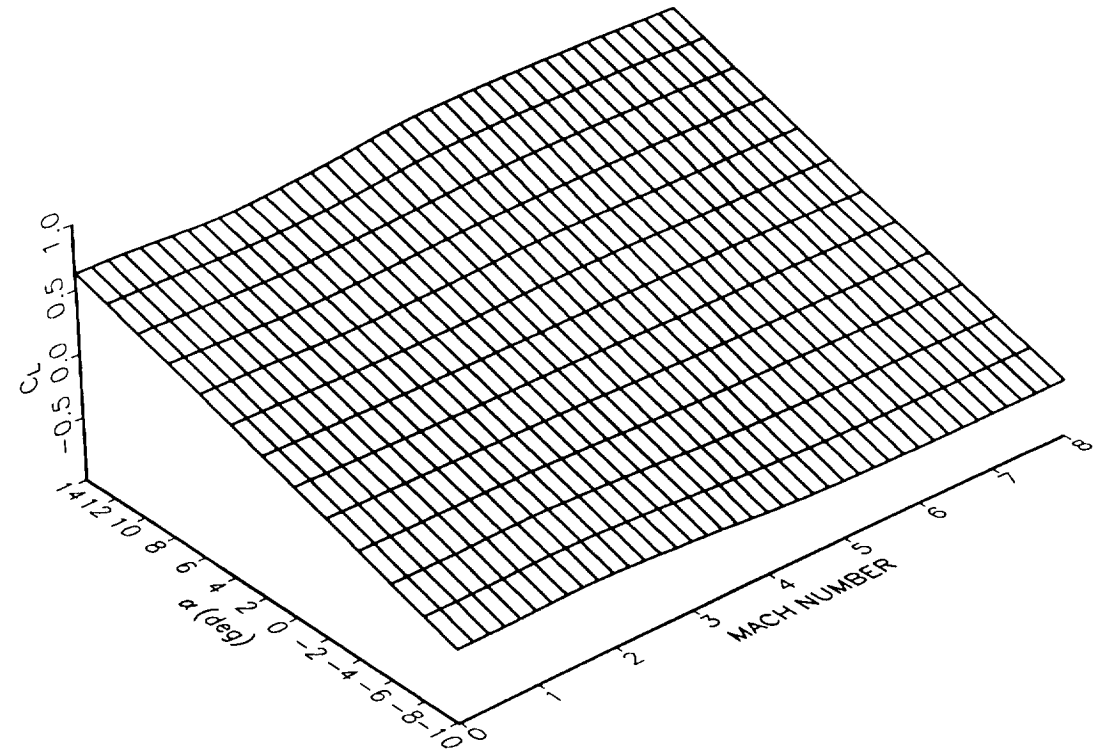

Figure 12: Lift Coefficient Surface Plot

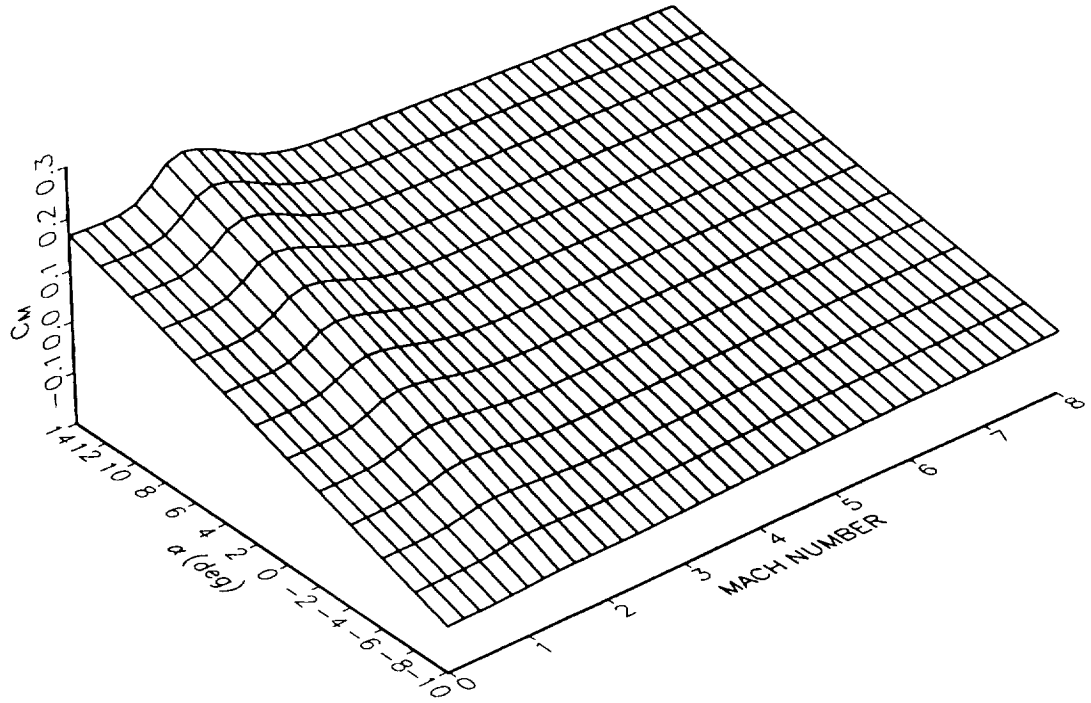

Figure 13: Pitch Moment Coefficient Surface Plot

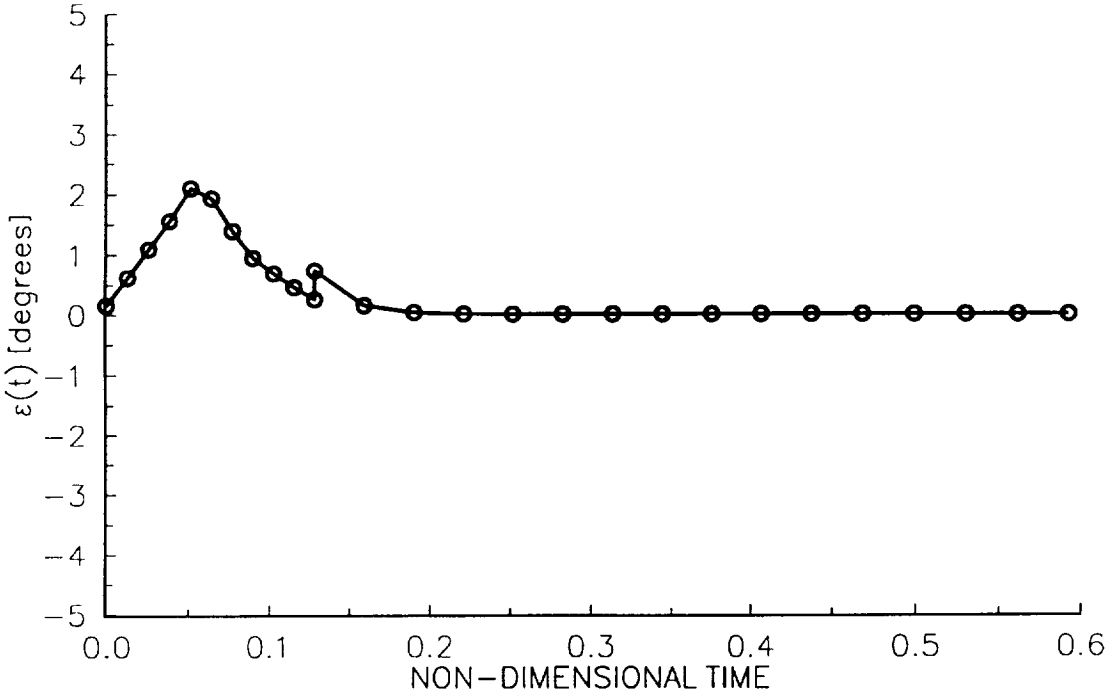

Figure 14: Control History, $\varepsilon(t)$, for Reduced Pitch Plane Solution

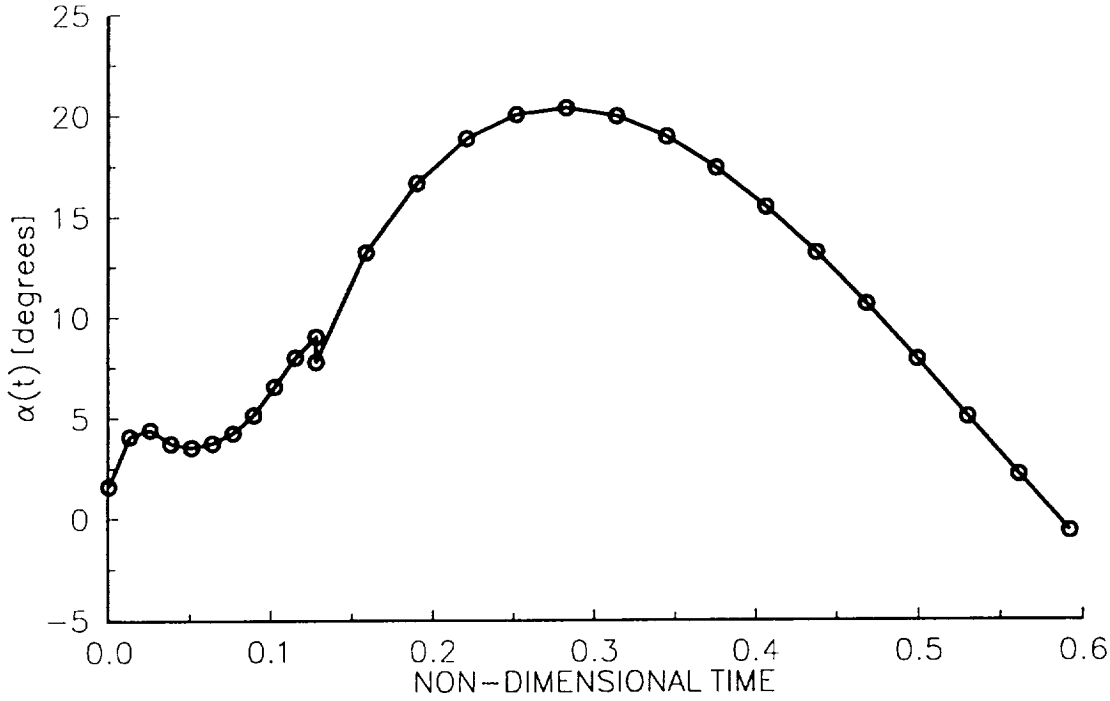

Figure 15: Control History, $\alpha(t)$, for Reduced Pitch Plane Solution

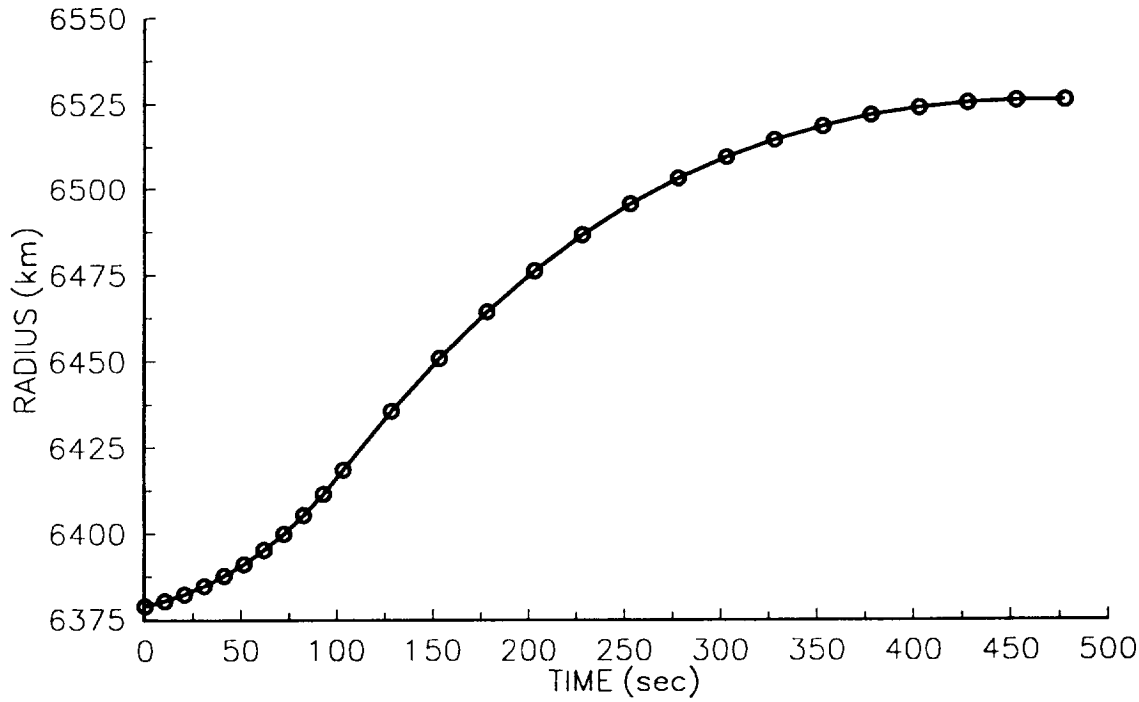

Figure 16: Radius History for Reduced Pitch Plane Solution

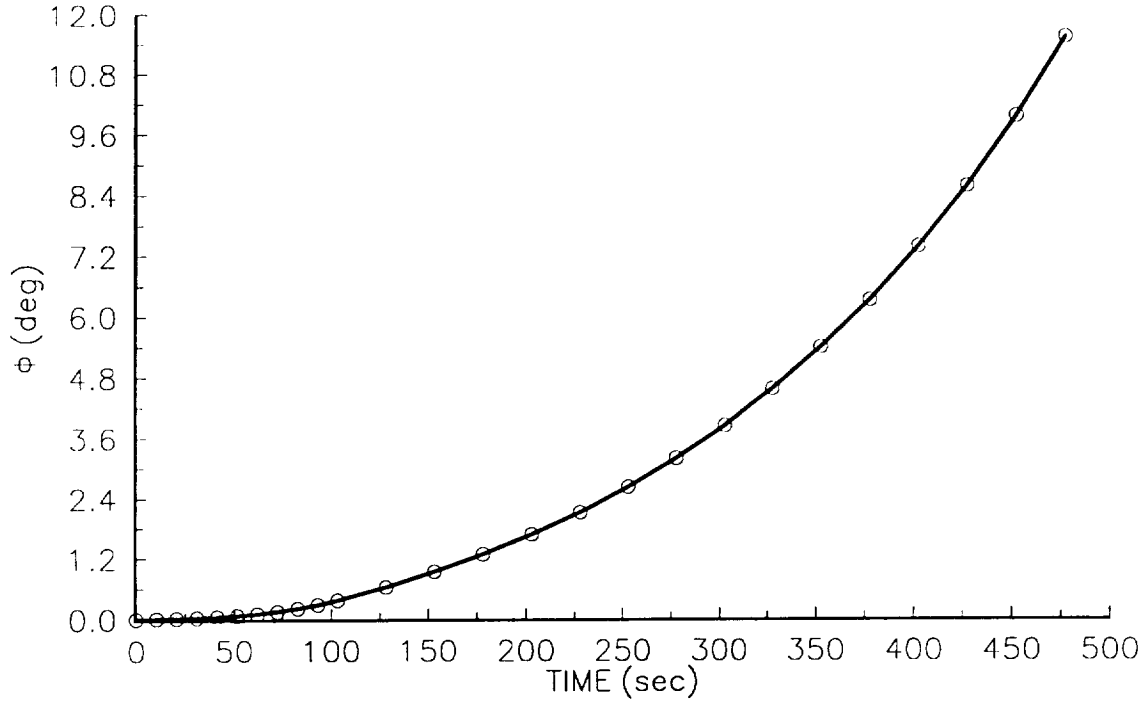

Figure 17: Downrange Angle for Reduced Pitch Plane Solution

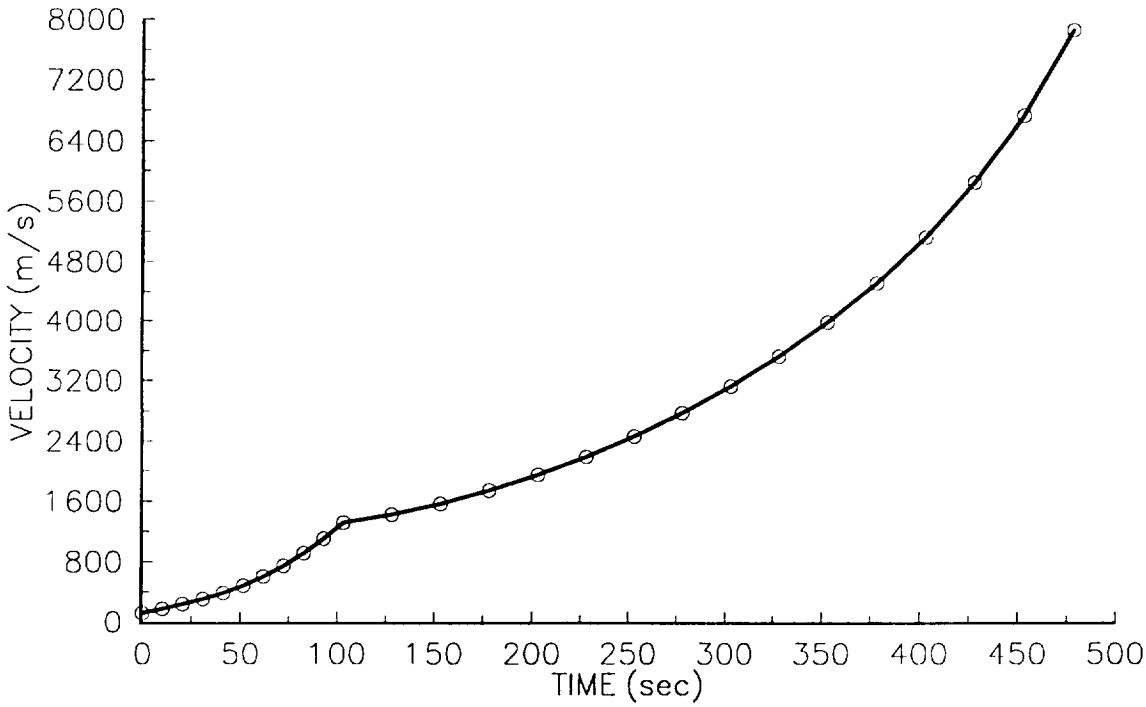

Figure 18: Velocity History for Reduced Pitch Plane Solution

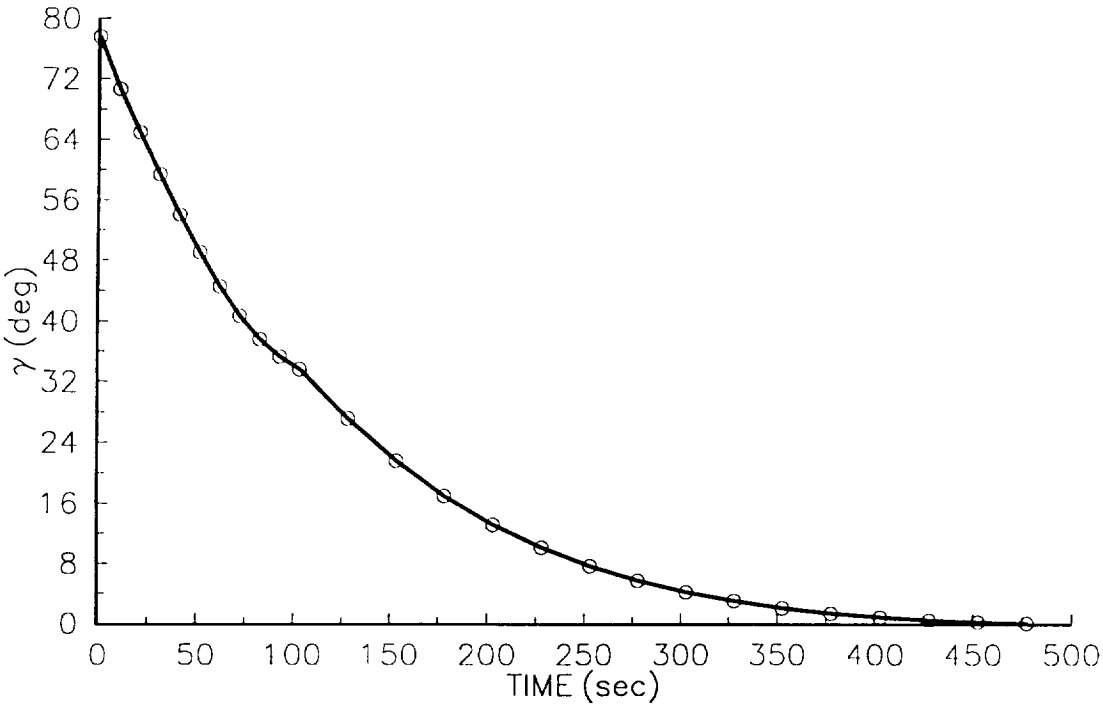

Figure 19: Flight Path Angle for Reduced Pitch Plane Solution

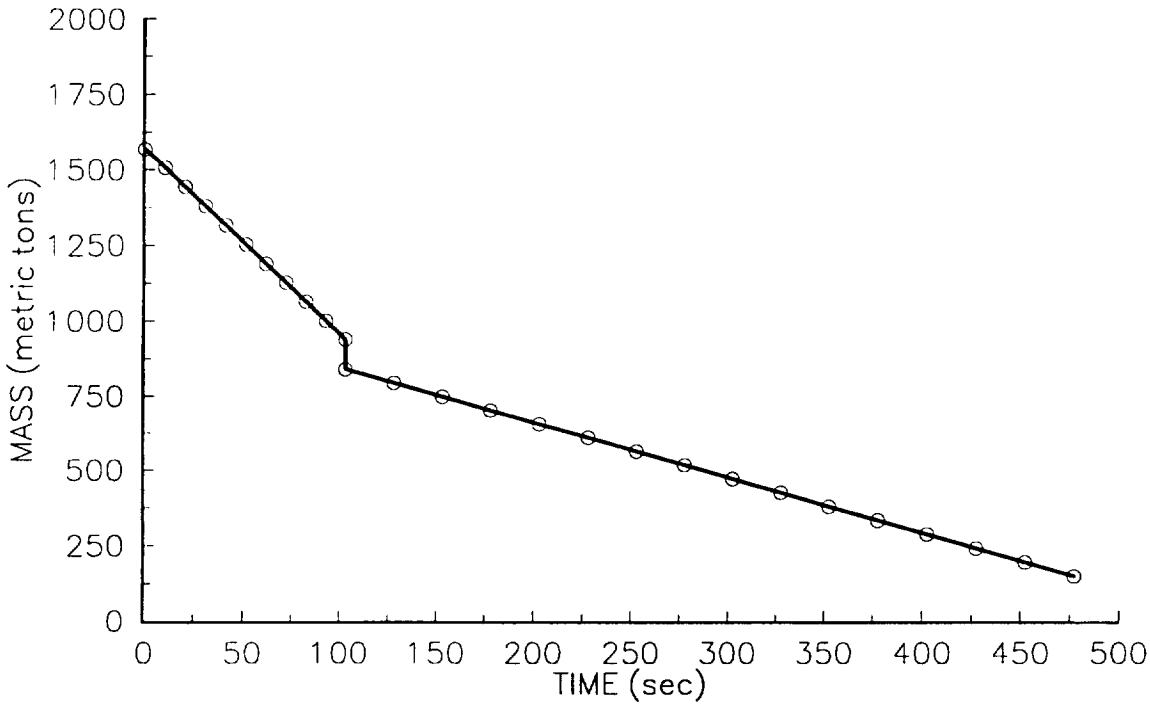

Figure 20: Vehicle Mass History for Reduced Pitch Plane Solution

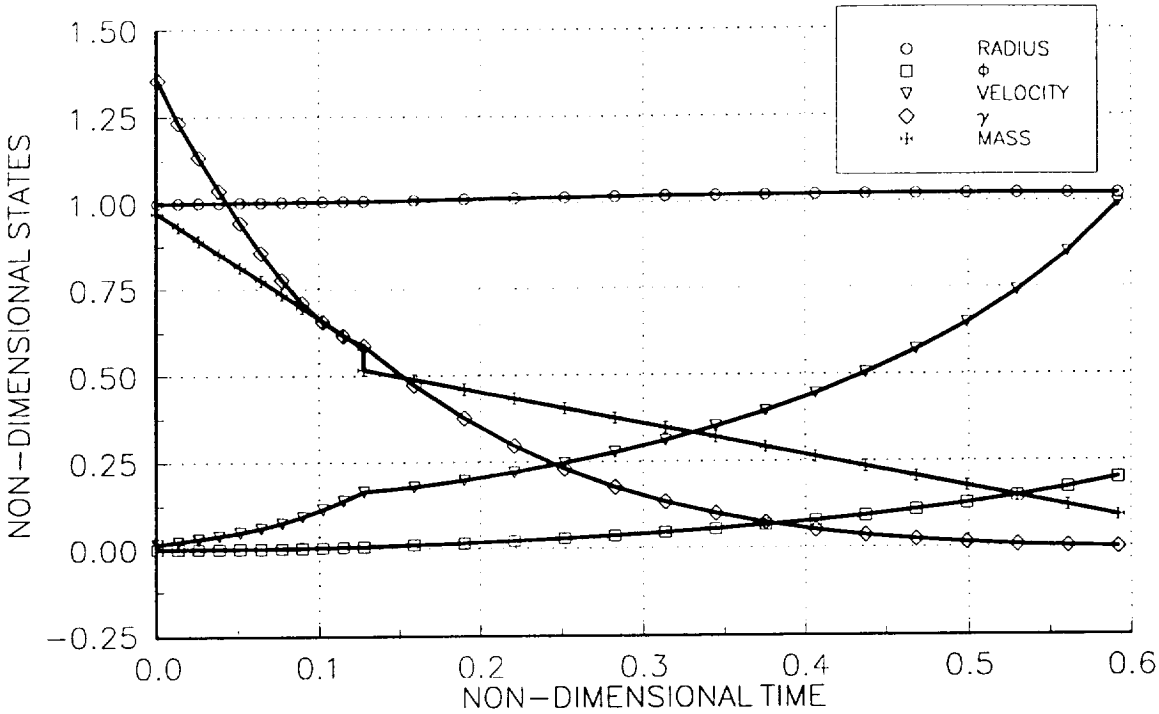

Figure 21: State Variables for Reduced Pitch Plane Solution

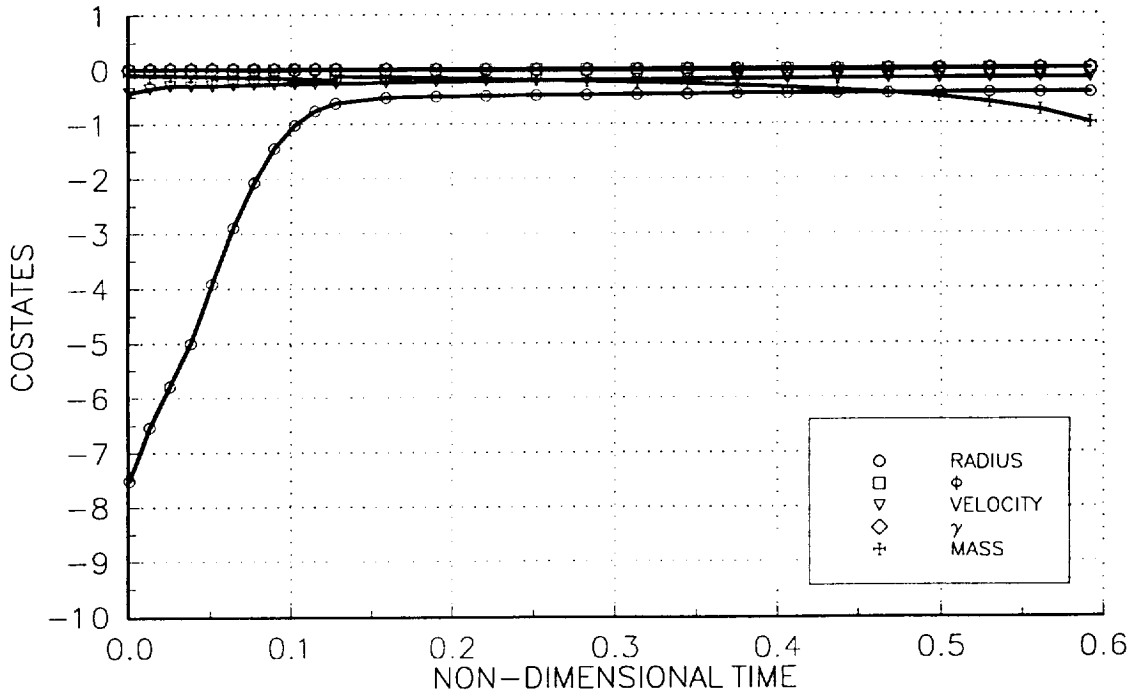

Figure 22: Costate Variables for Reduced Pitch Plane Solution